

molecule T22 suggests a convergence of innate and adaptive recognition strategies. G8, like $\alpha\beta$ TCRs and antibodies, uses its CDR loops to bind its ligand, T22. However, G8 almost exclusively uses its genetically recombined CDR3 δ loop to bind T22 from the side with degenerate contacts for the remaining CDR δ and CDR3 γ loops, suggesting that the CDR3 δ loop is the primary docking anchor in this recognition strategy. Moreover, the residues involved in the recognition interface are derived predominantly from germline-encoded D δ segments, suggesting that there is, as previously hypothesized, a germline-encoded basis for T10/T22 recognition. The additional use of junctionally diverse residues in the interface allows for rapid coevolution of $\gamma\delta$ TCRs with their ligands. This is an ideal strategy for an innate receptor, because there can be not only a long-term coevolution of the $\gamma\delta$ TCR and its ligand over the lifetime of a species but also an immediate fine-tuning of the recognition of its particular ligand within an individual. In this way, the chemistry of the recognition interface between G8 and T22 can be thought of as a hybrid between innate and adaptive recognition solutions.

References and Notes

- A. C. Hayday, *Annu. Rev. Immunol.* **18**, 975 (2000).
- Y. H. Chien, R. Jores, M. P. Crowley, *Annu. Rev. Immunol.* **14**, 511 (1996).
- M. M. Davis, P. J. Bjorkman, *Nature* **334**, 395 (1988).
- M. G. Rudolph, I. A. Wilson, *Curr. Opin. Immunol.* **14**, 52 (2002).
- E. P. Rock, P. R. Sibal, M. M. Davis, Y. H. Chien, *J. Exp. Med.* **179**, 323 (1994).
- C. T. Morita, R. A. Mariuzza, M. B. Brenner, *Springer Semin. Immunopathol.* **22**, 191 (2000).
- L. A. Matis, R. Cron, J. A. Bluestone, *Nature* **330**, 262 (1987).
- H. Schild *et al.*, *Cell* **76**, 29 (1994).
- M. P. Crowley *et al.*, *Science* **287**, 314 (2000).
- S. Shin *et al.*, *Science* **308**, 252 (2005).
- C. Wingren, M. P. Crowley, M. Degano, Y. Chien, I. A. Wilson, *Science* **287**, 310 (2000).
- M. G. Rudolph, C. Wingren, M. P. Crowley, Y. H. Chien, I. A. Wilson, *Acta Crystallogr. D Biol. Crystallogr.* **60**, 656 (2004).
- Materials and methods are available as supporting material on Science Online.
- T. J. Allison, C. C. Winter, J. J. Fournie, M. Bonneville, D. N. Garboczi, *Nature* **411**, 820 (2001).
- S. R. Carding *et al.*, *J. Exp. Med.* **172**, 1225 (1990).
- E. J. Sundberg, Y. Li, R. A. Mariuzza, *Curr. Opin. Immunol.* **14**, 36 (2002).
- K. C. Garcia *et al.*, *Science* **274**, 209 (1996).
- D. N. Garboczi *et al.*, *Nature* **384**, 134 (1996).
- I. A. Wilson, K. C. Garcia, *Curr. Opin. Struct. Biol.* **7**, 839 (1997).
- P. Li *et al.*, *Immunity* **10**, 577 (1999).
- P. Li *et al.*, *Nat. Immunol.* **2**, 443 (2001).
- E. O. Saphire *et al.*, *Science* **293**, 1155 (2001).
- R. L. Stanfield, H. Dooley, M. F. Flajnik, I. A. Wilson, *Science* **305**, 1770 (2004).
- L. A. Matis, J. A. Bluestone, *Semin. Immunol.* **3**, 75 (1991).
- K. C. Garcia *et al.*, *Science* **279**, 1166 (1998).
- E. L. Reinherz *et al.*, *Science* **286**, 1913 (1999).
- Z. Reich *et al.*, *Nature* **387**, 617 (1997).
- W. Haas, P. Pereira, S. Tonegawa, *Annu. Rev. Immunol.* **11**, 637 (1993).
- S. M. Hayes, P. E. Love, *Immunity* **16**, 827 (2002).
- Y. H. Chien, J. Hampl, *Springer Semin. Immunopathol.* **22**, 239 (2000).
- D. Kabelitz, D. Wesch, *Crit. Rev. Immunol.* **23**, 339 (2003).
- Y. Li, H. Li, F. Yang, S. J. Smith-Gill, R. A. Mariuzza, *Nat. Struct. Biol.* **10**, 482 (2003).
- W. L. Delano, Delano Scientific, San Carlos, CA, USA, 2002.
- We thank M. Boulanger, P. Strop, and S. Shin for advice and helpful discussions. We also acknowledge Stanford Synchrotron Radiation Laboratory and Advanced Light Source for x-ray resources. This work was supported by a Cancer Research Institute Postdoctoral Fellowship (E.J.A.), an NIH-Immunology postdoctoral training grant (E.J.A.), the Keck Foundation, and NIH (AI048540) (K.C.G.). Coordinates of the asymmetric unit have been deposited in the Protein Data Bank with accession code 1YPZ (RCSB031793).

Supporting Online Material

www.sciencemag.org/cgi/content/full/308/5719/227/DC1

Materials and Methods

Fig. S1

Tables S1 to S5

28 October 2004; accepted 9 February 2005

10.1126/science.1106885

REPORTS

The Real-Time Stellar Evolution of Sakurai's Object

Marcin Hajduk,^{1,2} Albert A. Zijlstra,^{1*} Falk Herwig,³
Peter A. M. van Hoof,^{4,5} Florian Kerber,⁶ Stefan Kimeswenger,⁷
Don L. Pollacco,⁴ Aneurin Evans,⁸ José A. López,⁹
Myfanwy Bryce,¹⁰ Stewart P. S. Eyres,¹¹ Mikako Matsuura¹

After a hot white dwarf ceases its nuclear burning, its helium may briefly and explosively reignite. This causes the star to evolve back into a cool giant, whereupon it experiences renewed mass ejection before reheating. A reignition event of this kind was observed in 1996 in V4334 Sgr (Sakurai's object). Its temperature decrease was 100 times the predicted rate. To understand its unexpectedly fast evolution, we have developed a model in which convective mixing is strongly suppressed under the influence of flash burning. The model predicts equally rapid reheating of the star. Radio emission from freshly ionized matter now shows that this reheating has begun. Such events may be an important source of carbon and carbonaceous dust in the Galaxy.

Helium-shell flashes play a vital role in the production of chemical elements in stars (1). They occur in all stars with initial masses between 1 and 8 times the mass of the Sun, during their asymptotic giant branch (AGB) phase. This phase ends with a drastic and rather sudden episode during which up to 90% of the star's mass is ejected into space. The remnant star evolves through a hot state toward the white dwarf cooling track, where nuclear burning ceases. Its radiation ionizes

the ejected material and a planetary nebula forms. About one-quarter of these stars will undergo one final, very late He flash as a white dwarf, after nuclear hydrogen burning has ceased (1–3), in a unique event of nuclear flash-driven stellar evolution. The reincarnated star retraces its evolution and experiences renewed mass ejection.

The discovery of Sakurai's object (V4334 Sgr) in 1996 provided the first modern observations of this so-called very late thermal pulse

(4). Its real-time evolution (possibly the fastest ever observed) provides a once-in-a-lifetime observational handle on the physics of convection and rapid nuclear burning. V4334 Sgr was the hot (10^5 K) central star of a hitherto undetected planetary nebula (5). Shortly before 1995, the helium layer reignited and V4334 Sgr was reincarnated as a “born-again” giant.

In our Galaxy, such an event is expected to occur once per decade (6). But V4334 Sgr was only the third observed case, after V605 Aql in 1918 (7) and possibly CK Vul in 1670 (8). Other events, such as the eruption of FG Sge (9), may have been missed in the crowded regions of the Milky Way. Hydrogen-poor [WC] central stars of planetary nebulae and the cooler hydrogen-deficient and carbon-rich R CrB stars (10) may be descendants of the born-again stars.

Computer simulations of the very late He-shell flash show that the small remaining H-rich envelope is convectively ingested into the He shell, resulting in an additional rapid H-driven nuclear flash burning. Initial models predicted that the stellar luminosity would increase, and temperature decrease, over a few hundred years (1, 2). However, V4334 Sgr evolved at 100 times the predicted rate, suggesting neglected physics in the simulations (11, 12). During 1998, increasing opacity by a dusty wind (13) rendered V4334 Sgr all but unobservable in the visual region. The mass

loss rate increased to 1.6×10^{-5} solar masses per year in 2001 (14). Indications for ionization were found in 2002 (15), suggesting that the star may be starting to reheat already.

To directly detect the renewed ionization, we observed Sakurai's object with the Very Large Array (VLA) on 5 February 2004. Optical images of O^{2+} emission were obtained using the focal reducer FORS1 on the ESO 8-m Very Large Telescope on 2 October 2002 (16). The image is shown in Fig. 1, with the VLA 8.6-GHz radio contours superposed. It shows the old planetary nebula (the extended shell) and a central radio source, marginally resolved, which has no O^{2+} counterpart. We identify this central source with the emerging ionized core around the reheating central star.

Radio observations carried out in November 1998 did not show emission near the central star (17). This suggests that a considerable increase in emission has recently occurred in this region and shows that the star has begun to reheat. Thus, we are witnessing the nascent stages of the formation of a new planetary nebula. The actual formation of such an H-poor planetary nebula has never before been observed. V605 Aql formed a compact H-poor emission nebula after the 1919–1924 outburst, but its formation was not observed; like V4334 Sgr, it became enshrouded in an envelope of dust that rendered it invisible to the astronomical tools of 1920 and was only recovered 60 years later (18).

The inset of Fig. 1 shows an image obtained in 2001 by the Hubble Space Telescope (HST) at a wavelength of 814 nm. The radio core of the newly formed ionized region is shown superposed as contours. The radio core has an integrated 8.6-GHz flux of $100 \pm 30 \mu\text{Jy}$. The uncertainty is due to the variable nebular background. Gaussian fitting to the radio core gave a nominal deconvolved full width at half maximum (FWHM) size of 2.4×0.8 arc sec at a position angle of 170° . The radio core shows an

indication of a double structure, but this has not been confirmed. Bipolarity is observed in the H-poor ejecta for the born-again objects A30 and A78 and in V605 Aql (19, 20). Bipolarity could be caused in such very late He-flash objects by stellar rotation and/or a magnetic field.

We assume a distance to V4334 Sgr of 2 kpc (21, 22). Early infrared spectra show a wind velocity of 670 km/s in the helium line at 1080 nm, relative to the central star (23). With a time line of 10 years, this velocity corresponds to a diameter of 1.4 arc sec, consistent with the observed radio feature.

The time scales for the stellar evolution are determined by the depth below the surface where the reignition takes place. To reproduce the large discrepancy in time scales, our revised stellar evolution models (16) parametrically include the buoyancy effect of rapid nuclear burning on convective turbulence in the He-shell flash zone. This reduces the convective mixing efficiency (11) and accelerates the evolution, because nuclear energy from fast proton capture is released closer to the stellar surface. The models reproduce the carbon isotope ratios and can explain the observed production of lithium (16, 24). Models with suppressed mixing reproduced the fast cooling but predicted that V4334 Sgr would equally rapidly reheat (12, 25).

Figure 2 shows our track of past and predicted future evolution. A good fit for the recent evolution is obtained if we assume that the reignition occurred in 1992 (the fast brightening in early 1995 can be explained by the rapid temperature evolution). The current detection of radio emission agrees with the predictions of

rapid reheating. Continued monitoring over the next few years is essential to further test the evolutionary predictions. Confirmation of the effect of suppressed mixing has important implications for the physics of convective turbulence under the influence of rapid nuclear burning.

The newly ejected nebula consists almost exclusively of helium and carbon with very little hydrogen. We modeled these with the use of the photoionization code Cloudy (16). Abundance ratios were taken as those of the stellar atmosphere just before the obscuration (24), with $C/He = 0.1$ and $H/He = 0.004$. The radio flux, size, and line ratios were fitted with a hydrogen density $n(H) = 36 \text{ cm}^{-3}$ and a dust-to-gas mass ratio of 3.9×10^{-2} . The electron temperature and density predicted by the model are shown in Fig. 3. The radial stratification of the most dominant ions causes a step-like decrease in the electron density. The N^+ diameter is smaller than the region of carbon ionization because of its higher ionization potential. The model predicts $N^+_{658.4 \text{ nm}}/H\alpha = 9.3$, in fair agreement with observations. The predicted ratio $O^+_{731.9+733.0}/N^+_{658.4 \text{ nm}} = 8.0 \times 10^{-4}$ is in disagreement with the observed ratio of unity (14): The electron temperature is insufficient to excite the upper levels of the O^+ transitions. The detected O^+ lines may be shock excited, or the presence of large amounts of very small grains [as found in V605 Aql (26)] could lead to higher photoelectric heating than in our current model. Shock ionization is also not included in the model. Shocks at the observed wind velocity would lead to O^{2+} that is not observed, but a differential wind speed on the order of 100 km/s (as would

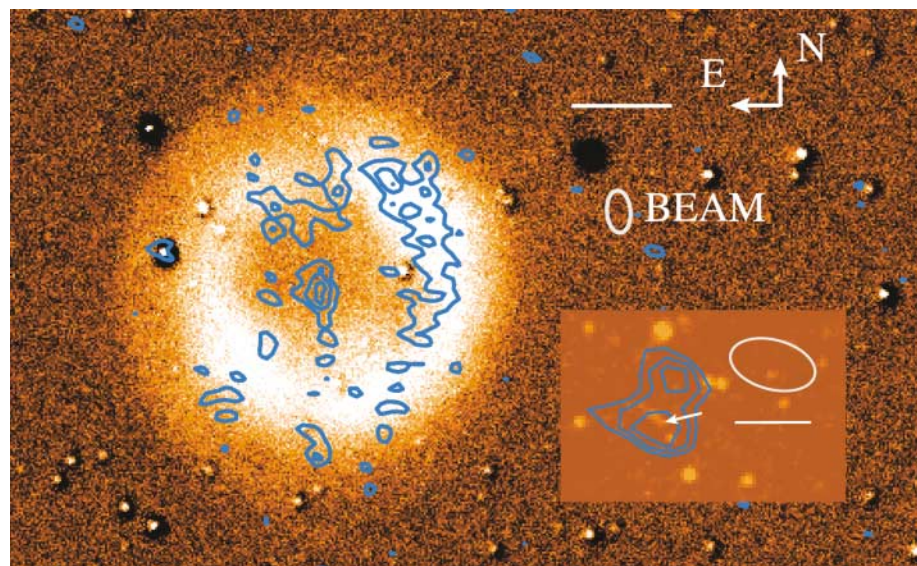


Fig. 1. Continuum-subtracted O^{2+} image showing the extended planetary nebula. Radio (8.6 GHz) contours are shown superposed at 30, 50, and 70 μJy per beam. A natural weighted map (beam of 4.2×2.4 arc sec indicated by the oval) is shown. Scale bar, 10 arc sec. (Inset) An HST I-band (F814W) image taken 29 August 2001. Sakurai's object (fainter of the two components, 0.2 arc sec apart) is indicated by an arrow. The superposed radio data show a uniform weighted map (beam of 2.2×1.3 arc sec, indicated by the oval) with contours at 25, 35, and 45 μJy per beam. The old planetary nebula is 41 arc sec in diameter; its brighter inner ring is 29 arc sec across. Scale bar, 2 arc sec.

¹School of Physics and Astronomy, University of Manchester, Post Office Box 88, Manchester M60 1QD, UK.

²Centrum Astronomii UMK, ul. Gagarina 11, PL-87-100 Torun, Poland.

³Theoretical Astrophysics Group T-6, Los Alamos National Laboratory, MS B227, Los Alamos, NM 87545, USA.

⁴APS Division, Department of Physics and Astronomy, Queen's University Belfast, Belfast BT7 1NN, UK.

⁵Royal Observatory of Belgium, Ringlaan 3, Brussels, Belgium.

⁶Space Telescope European Coordinating Facility, European Southern Observatory (ESO), Karl-Schwarzschild-Strasse 2, 85748 Garching, Germany.

⁷Institut für Astrophysik, Universität Innsbruck, Technikerstr. 25, 6020 Innsbruck, Austria.

⁸Department of Physics, School of Chemistry and Physics, Keele University, Staffordshire ST5 5BG, UK.

⁹Instituto de Astronomía, Universidad Nacional Autónoma de México, Apdo. Postal 877, 22800 Ensenada, BC, Mexico.

¹⁰Jodrell Bank Observatory, School of Physics and Astronomy, University of Manchester, Macclesfield, Cheshire SK11 9DL, UK.

¹¹Centre for Astrophysics, University of Central Lancashire, Preston PR1 2HE, UK.

*To whom correspondence should be addressed.

E-mail: a.zijlstra@manchester.ac.uk

be expected if the star were reheating) could lead to O⁺ formation.

The model predicts an ionized mass of 1.0×10^{-3} solar masses, mainly consisting of singly ionized carbon. Including the neutral mass within the ionized region yields 2×10^{-3} solar masses, where we use the mass ratio $X(C)/X(He) \sim 1$ corresponding to the model predictions (11). The dust mass is 1.85×10^{-4} solar masses. The total mass of the shell implies a mass loss rate of 2×10^{-4} solar masses per year. The observed mass loss rates have increased over time but reached only $\sim 10^{-5}$ in 2001 (14). This discrepancy may indicate that the shell is clumped, which would reduce our mass determination.

We find that Sakurai's object ejected about 5×10^{-4} solar masses of primary carbon, of which roughly 20% is located in the dust. Interstellar carbon dust comes mainly from AGB stars with C/O ratios above unity. In metal-rich populations, such as the inner Galaxy, this is reached in very few stars, and here Sakurai-type events may give an important contribution. V4334 Sgr shows a very high ratio of $^{13}C/^{12}C = 0.2$ (27) relative to the interstellar abundance ratio of 0.01. Together with novae (28), born-again giants may be the dominant ^{13}C source in the universe. Traces of this unique kind of mass ejecta may have been found in primitive meteorites. Isotopic analysis of presolar SiC A+B grains extracted from a

sample of the Murchison carbonaceous meteorite are characterized by having $^{12}C/^{13}C < 10$. A subset of these grains also show enrichment of elements produced by slow neutron capture (s-process), and an origin in nuclear flash objects such as V4334 Sgr has been suggested (29). Our observations provide a quantitative estimate of the carbon mass lost in a born-again evolution and strengthen the possible link to presolar meteoritic grains.

References and Notes

1. M. A. Fujimoto, *Publ. Astron. Soc. Jpn.* **29**, 331 (1977).
2. F. Herwig, T. Bloeker, N. Langer, T. Driebe, *Astron. Astrophys.* **349**, L5 (1999).
3. I. Iben Jr., J. MacDonald, *Lect. Notes Phys.* **443**, 48 (1995).
4. H. W. Duerbeck, S. Benetti, *Astrophys. J.* **468**, L111 (1996).
5. F. Kerber, J. Köppen, M. Roth, S. C. Trager, *Astron. Astrophys.* **344**, L79 (1999).
6. A. A. Zijlstra, *Astrophys. Space Sci.* **279**, 171 (2002).
7. M. Lechner, S. Kimeswenger, *Astron. Astrophys.* **426**, 145 (2004).
8. A. Evans *et al.*, *Mon. Not. R. Astron. Soc.* **332**, L35 (2002).
9. T. Bloeker, D. Schoenberner, *Astron. Astrophys.* **324**, 991 (1997).
10. G. C. Clayton, *Publ. Astron. Soc. Pac.* **108**, 225 (1996).
11. F. Herwig, *Astrophys. J.* **554**, L71 (2001).
12. T. M. Lawlor, J. MacDonald, *Astrophys. J.* **583**, 913 (2003).
13. M. Asplund, B. Gustafsson, D. L. Lambert, R. N. Kameswara, *Astron. Astrophys.* **321**, L17 (1997).
14. V. H. Tyne *et al.*, *Mon. Not. R. Astron. Soc.* **334**, 875 (2002).
15. F. Kerber *et al.*, *Astrophys. J.* **581**, L39 (2002).
16. See supporting data on Science Online.
17. S. P. S. Eyres, *Astrophys. Space Sci.* **279**, 69 (2002).
18. W. C. Seitter, *ESO Messenger* (no. 50), 14 (1987).
19. J. Meaburn, J. A. Lopez, M. Bryce, *Astron. Astrophys.* **334**, 670 (1998).
20. K. Hinkle *et al.*, in *Exotic Stars as Challenges to Evolution*, C. A. Tout, W. Van Hamme, Eds. (ASP Conference Proceedings 279, Astronomical Society of the Pacific, San Francisco, 2002), p. 187.
21. S. Kimeswenger, *Astrophys. Space Sci.* **279**, 79 (2002).
22. A. Evans, T. R. Geballe, B. Smalley, V. H. Tyne, S. P. S. Eyres, *Astron. Astrophys.* **394**, 971 (2002).
23. S. P. S. Eyres *et al.*, *Mon. Not. R. Astron. Soc.* **307**, L11 (1999).
24. M. Asplund, D. L. Lambert, T. Kipper, D. Pollacco, M. D. Shetrone, *Astron. Astrophys.* **343**, 507 (1999).
25. F. Herwig, in *Planetary Nebulae: Their Evolution and Role in the Universe*, S. Kwok, M. Dopita, R. Sutherland, Eds. (IAU Symposium 209, Astronomical Society of the Pacific, San Francisco, 2003), p. 111.
26. J. Koller, S. Kimeswenger, *Astrophys. J.* **559**, 419 (2001).
27. Y. V. Pavlenko *et al.*, *Astron. Astrophys.* **417**, L39 (2004).
28. D. Romano, F. Matteucci, *Mon. Not. R. Astron. Soc.* **342**, 185 (2003).
29. S. Amari, L. R. Nittler, E. Zinner, K. Lodders, R. S. Lewis, *Astrophys. J.* **559**, 463 (2001).
30. Supported by the EU Marie Curie Training Site program under contract HPMT-CT-2000-00069 (M.H.), Los Alamos National Laboratory under U.S. Department of Energy contract W-7405-ENG-36 (F.H.), the UK Engineering and Physical Sciences Research Council (P.A.M.v.H.), the UK Particle Physics and Astronomy Research Council (M.M.), an extended-visit grant to the UK from the Royal Society and the Academia Mexicana de Ciencias (J.A.L.), and the Nuffield Foundation (S.P.S.E.). The photoionization code Cloudy can be obtained from www.nublado.org. The observations described above made use of the Very Large Array, operated by the National Radio Astronomy Observatory, and the ESO Very Large Telescope.

Supporting Online Material
www.sciencemag.org/cgi/content/full/308/5719/231/DC1
 Materials and Methods
 References

21 December 2004; accepted 18 February 2005
 10.1126/science.1108953

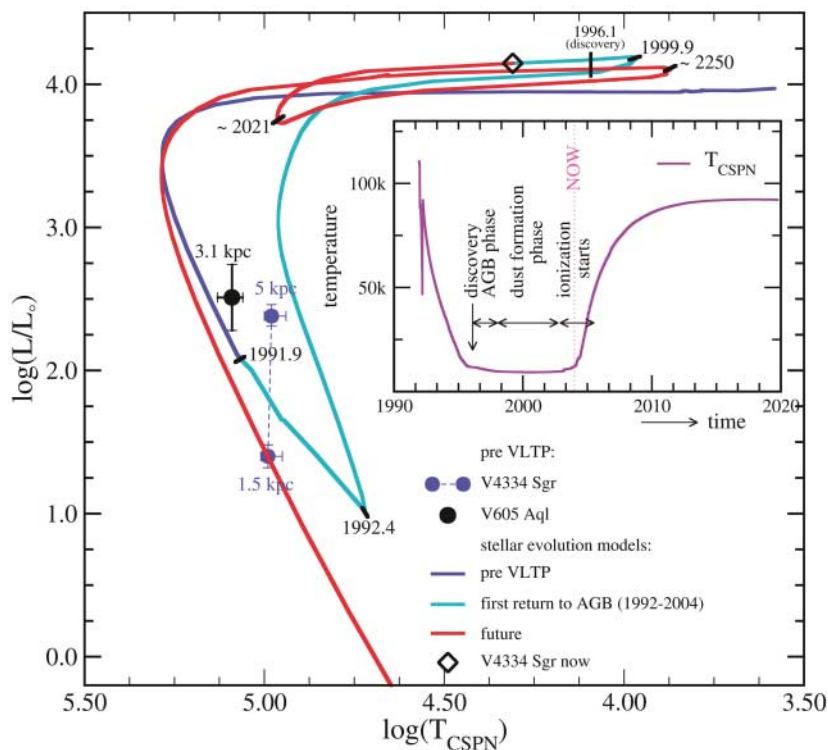


Fig. 2. Stellar model sequence of the past and future temperature and luminosity evolution of Sakurai's object. Two loops are predicted; the first loop corresponds to the hydrogen ingestion flash, and the second, much slower loop corresponds to the helium flash. Predicted times for past and future extrema are indicated. In this model, Sakurai's object is currently at the start of a fast temperature increase. The preflash positions of V4334 Sgr and V605 Aql are based on the ionization structure of their old nebulae (5, 7).

Fig. 3. The physical conditions predicted by the Cloudy model. T_e , electron temperature; n_e , electron density.

